HOSTED BY

ELSEVIER

Available online at www.sciencedirect.com

ScienceDirect

journal homepage: http://ees.elsevier.com/ejbas/default.asp

Enhancement of TiO_2-photocatalyzed organic transformation by ZnO and ZnS. Oxidation of diphenylamine

C. Karunakaran [*], *S. Karuthapandian* [1]

Department of Chemistry, Annamalai University, Annamalainagar 608002, Tamilnadu, India

ARTICLE INFO

Article history:
Received 4 September 2014
Received in revised form
22 October 2014
Accepted 3 December 2014
Available online 19 December 2014

Keywords:
Photocatalysis
Semiconductor
Kinetic law
Interparticle charge transfer

ABSTRACT

TiO_2 anatase photocatalyzes the oxidative transformation of diphenylamine (DPA) to N-phenyl-*p*-benzoquinonimine (PBQ) in ethanol. The PBQ formation increases with increase of [DPA], TiO_2-loading, airflow rate and light intensity. The catalyzed formation of PBQ is larger with UV-C light illumination than with UV-A light illumination. The catalyst is recyclable. The photocatalytic reaction mechanism has been proposed and the kinetic parameters deduced. ZnO and ZnS enhance the TiO_2-photocatalyzed DPA oxidation suggesting interparticle charge transfer in mixed semiconductors.

1. Introduction

Semiconductor-photocatalysis for environmental cleanup has been extensively studied [1,2] and reports on the application of this process for selective organic transformations are also available [3–5]. The photocatalytic technology is benign and TiO_2 is widely employed as a photocatalyst for both applications [2,3,5]. On band gap excitation, TiO_2 produces electron–hole pairs; electrons in the conduction band (CB) and holes in the valence band (VB) [2]. In the presence of moisture and air, the photoproduced charge carriers generate reactive oxidizing species (ROS) such as hydroxyl radical, which mineralize the organic pollutants. The VB hole oxidizes the water molecule and hydroxide ion adsorbed on the TiO_2 surface to produce hydroxyl radical. The oxygen molecule adsorbed on TiO_2 picks up the CB electron to form superoxide radical, which through a series of reactions yield hydroxyl radical. But in non-aqueous media formation of hydroxyl radical is unlikely and the VB hole directly oxidizes the adsorbed substrate and hence photocatalyzed organic transformations are carried out in non-aqueous media. TiO_2 selectively oxidizes alcohols to aldehydes or ketones and functionalized nitroarenes are selectively reduced by N-doped TiO_2 [4]. Propene and cyclopentene are transformed into the corresponding epoxide using TiO_2–SiO_2 as photocatalyst [4]. TiO_2 Degussa P25 selectively photocatalyzes the oxidation of benzyl amines to the corresponding imines [5]. However, significant amounts of aldehydes are produced on the

* *Corresponding author*. Tel.: +91 9443481590; fax: +91 4144238145.
E-mail address: karunakaranc@rediffmail.com (C. Karunakaran).
Peer review under responsibility of Mansoura University.
[1] Present address: Department of Chemistry, VHNSN College, Virudhunagar 626001, Tamilnadu, India.
http://dx.doi.org/10.1016/j.ejbas.2014.12.001

photooxidation of secondary benzyl amines on TiO_2 [5]. TiO_2 is also useful for the photocatalytic oxidative dehydrogenation of 1,2,3,4-tetrahydroquinoline [5]. Diphenylamine (DPA) is widely used in post-harvest treatment of apple and pear [6] and there is no study on the photocatalytic transformation of DPA. Photosensitized oxidation of DPA has been reported and cyanoanthracenes [7] and benzophenone [8] are some of the photosensitizers used. Photolysis of DPA solution in ethanol slowly yields N-phenyl-*p*-benzoquinonimine (PBQ) [9]. Hence it is of interest to study the photocatalytic transformation of DPA with nanocrystalline TiO_2 anatase. Generally, the photocatalytic activity could be improved by enhancing the lifetime of the charge carriers in semiconductor nanoparticles. This could be achieved through interparticle charge transfer (IPCT). When a mixture of two nanoparticulate semiconductors is used as a photocatalyst for mineralization of organics enhanced photocatalytic activity has been observed [10,11]. This has been explained on the basis of IPCT. However, such enhancement is not realized in the photocatalytic oxidation of iodide ion suggesting the IPCT to be slower than hole-transfer to iodide ion [12]. Hence it is of interest to study photocatalytic organic transformation using nanoparticulate semiconductor mixture as photocatalyst. Here we investigate the photocatalytic transformation of DPA on TiO_2 and TiO_2–ZnO and TiO_2–ZnS mixtures; ZnO has also been employed as photocatalyst for organic transformation [5]. Systematic study on TiO_2-photocatalyzed transformation of DPA has been made to deduce the kinetic law of the reaction. TiO_2 acts as a photocatalyst under natural sunlight utilizing the UV light (5%) present in the solar spectrum and hence the reaction has also been examined with natural sunlight.

2. Experimental procedure

2.1. Materials and measurements

TiO_2, ZnS and ZnO (Merck) were used as supplied and their specific surface areas, obtained by BET method, are 14.7, 7.7 and 12.2 $m^2\ g^{-1}$, respectively. The mean particle sizes (t) of TiO_2, ZnS and ZnO, deduced using the relationship $t = 6/\rho S$, where ρ is the material density and S is the specific surface area, are 104, 190 and 87 nm, respectively. The UV–visible diffuse reflectance spectra of the semiconductors were obtained using a Shimadzu UV-2600 spectrophotometer with an ISR-2600 integrating sphere attachment. The Kubelka–Munk plots provide the band gap energies of TiO_2, ZnS and ZnO as 3.18, 3.57 and 3.15 eV, respectively. The recorded powder X-ray diffractograms of TiO_2, ZnS and ZnO show the crystalline structures as anatase, zinc blende and wurtztie, respectively [13]. Potassium tris(oxalato)ferrate(III), $K_3[Fe(C_2O_4)_3].3H_2O$, was prepared following the reported procedure [14]. DPA, AR (Merck) was used as received. Commercial ethanol was distilled with calcium oxide.

2.2. Photocatalysis with UV light

Photocatalytic oxidation with UV light was performed in a multilamp photoreactor. The reactor was equipped with eight 8 W mercury UV lamps (Sankyo Denki, Japan) of wavelength 365 nm. The lamps were shielded by highly polished anodized aluminum reflector. Four cooling fans fixed at the bottom of the reactor dissipate the heat produced. A borosilicate glass tube of 15-mm inner diameter was used as the reaction vessel and was placed at the center of the photoreactor. The photoreaction was also carried out in a micro photoreactor fixed with a 6 W 254 nm low-pressure mercury lamp and a 6 W 365 nm mercury lamp. Quartz and borosilicate glass tubes were employed as reaction vessels for 254 and 365 nm lamps, respectively. The light intensity (I) was determined using ferrioxalate actinometer. The volume of the DPA solution was always maintained as 25 mL in the multilamp photoreactor and 10 mL in the micro-photoreactor. Air was bubbled through the DPA solution to keep the photocatalyst powder under suspension and at constant motion. The airflow rate was determined by soap bubble method. The UV–visible spectra were recorded using a Hitachi U-2001 UV–visible spectrophotometer, after diluting the solution 5-times to keep the

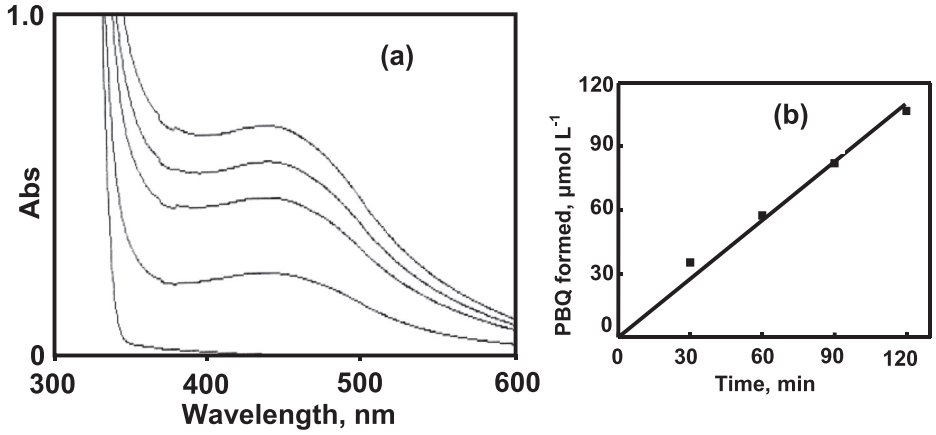

Fig. 1 – (a) PBQ formation in presence of TiO_2 under UV light in ethanol: the UV–visible spectra of reaction solution (5-times diluted) at 0, 30, 60, 90 and 120 min (↑) ([DPA] = 20 mM, TiO_2-loading = 1.0 g, airflow rate = 7.8 mL s^{-1}, I = 25.2 μeinstein $L^{-1}\ s^{-1}$, volume of reaction solution = 25 mL), (b) Linear increase of PBQ formed with illumination time.

absorbance within the Beer–Lambert law limit. The formed PBQ was estimated from its absorbance at 450 nm.

2.3. *Photocatalysis with sunlight*

The photocatalytic transformation with natural sunlight was made in summer (March–July) under clear sky at 11.30 am – 12.30 pm. The intensity of sunlight (W m^{-2}) was determined with a Global pyranometer, supplied by Industrial Meters, Bombay. The solar irradiance (Einstein L^{-1} s^{-1}) was also measured by ferrioxalate actinometry. The measured 440 W m^{-2} corresponds to 22 μEinstein L^{-1} s^{-1}. For each set of experiment, solution of DPA of desired concentration in ethanol was prepared afresh and taken in wide cylindrical glass vessels of uniform diameter. The entire bottom of the vessel was covered by the catalyst powder. Air was bubbled using a micro pump without disturbing the catalyst bed. The volume of DPA solution was 25 mL and the loss of solvent due to evaporation was compensated periodically. The formed PBQ was estimated spectrophotometrically.

3. Results and discussion

3.1. *TiO_2-catalyzed DPA oxidation with UV light*

The TiO_2-photocatalyzed oxidation of DPA in ethanol was carried out in the presence of air with a multilamp photoreactor fixed with UV lamps of wavelength 365 nm. The UV–visible spectra of the illuminated solution, recorded at different reaction time, reveal the formation of PBQ (λ_{max} = 450 nm). Fig. 1 (a) displays the time scan. The illuminated solution is EPR silent indicating absence of formation of diphenylnitroxide. In addition, thin layer chromatographic analysis shows the formation of a single product. The illuminated DPA solution was evaporated after the separation of TiO_2 powder and the solid was dissolved in chloroform to develop the chromatogram on a silica gel G-coated plate using benzene as eluant. The PBQ formed was estimated from the measured absorbance at 450 nm using its molar extinction coefficient [15,16]. The linear increase of [PBQ] with illumination time, displayed in Fig. 1 (b), provides the initial rate of PBQ formation and the rates are reproducible to ±6%. The direct photooxidation of DPA, the photoformation of PBQ in the absence of TiO_2, is not negligible [9] and the rate of TiO_2-photocatalyzed PBQ formation was obtained by measuring the rates of PBQ formation in the presence and absence of TiO_2. Fig. 2 displays the increase of rate of TiO_2-photocatalyzed PBQ formation with [DPA]. The results are characteristic of Langmuir–Hinshelwood kinetics with respect to [DPA]. The increase of the amount of TiO_2 suspended in the DPA solution results in increased PBQ formation and the rate reaches a limit at high TiO_2-loading; Fig. 3 presents the results. Determination TiO_2-photocatalyzed reaction rate at different airflow rates shows enhancement of TiO_2-photocatalyzed transformation by oxygen and the dependence of the reaction rate on the airflow rate conforms to the Langmuir–Hinshelwood kinetic law. The results are displayed in Fig. 4. PBQ formation was also measured without bubbling air but the solution was not deoxygenated.

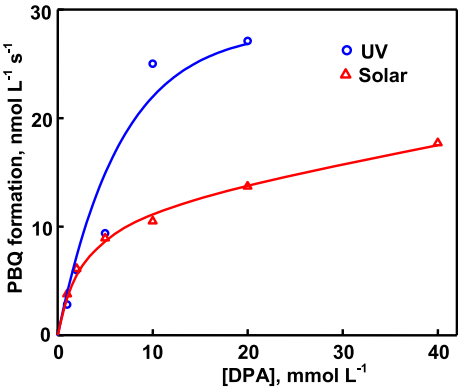

Fig. 2 – Dependence of TiO_2-photocatalyzed PBQ formation rate in ethanol on [DPA] (TiO_2-loading = 1.0 g, volume of reaction solution = 25 mL; UV: λ = 365 nm, I = 25.2 μeinstein L^{-1} s^{-1}, airflow rate = 7.8 mL s^{-1}; Solar: bed area = 11.36 cm^2, airflow rate = 4.6 mL s^{-1}).

The dissolved oxygen itself brings out the photocatalysis but the PBQ formation is slow. The TiO_2-catalyzed PBQ formation was examined at different light intensities. The reaction was carried out with two, four and eight lamps; the angles sustained by the adjacent lamps are 180°, 90° and 45°, respectively. Fig. 5 shows the variation of the catalyzed reaction rate with the light intensity. PBQ is not formed in the dark. Investigation of the TiO_2-catalyzed PBQ formation with UV-A and UV-C light, using a 6 W 365 nm mercury lamp (I = 18.1 μeinstein L^{-1} s^{-1}) and a 6 W 254 nm low-pressure mercury lamp (I = 5.22 μeinstein L^{-1} s^{-1}), separately in the micro-photoreactor under identical conditions reveals that UV-C light is more efficient than UV-A light in bringing out the organic transformation. PBQ formation with UV-A and UV-C light are 12.8 and 51.7 nmol L^{-1} s^{-1}, respectively. TiO_2 does not lose its photocatalytic activity on usage. Reuse of TiO_2 shows sustainable photocatalytic activity. Singlet oxygen quencher azide ion (5 mmol L^{-1}) fails to suppress the formation of PBQ indicating the absence of involvement of singlet oxygen in the photocatalytic transformation. This is in agreement with an earlier report; Fox and Chen [17] excluded

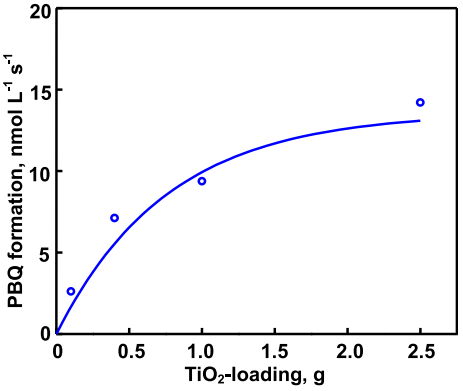

Fig. 3 – Variation of TiO_2-photocatalyzed PBQ formation rate in ethanol with TiO_2-loading ([PBQ] = 5.0 mM, airflow rate = 7.8 mL s^{-1}, λ = 365 nm, I = 25.2 μeinstein L^{-1} s^{-1}, volume of reaction solution = 25 mL).

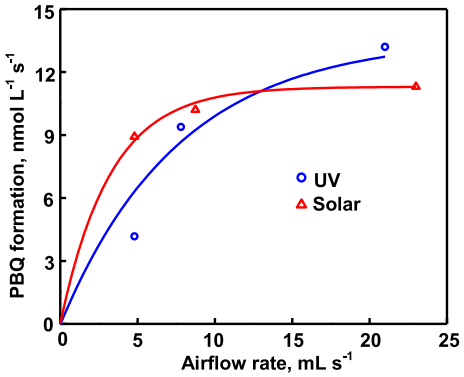

Fig. 4 – Influence of airflow rate on TiO_2-photocatalyzed PBQ formation rate ([DPA] = 5.0 mM, TiO_2-loading = 1.0 g, volume of reaction solution = 25 mL; UV: λ = 365 nm, I = 25.2 μeinstein L^{-1} s^{-1}; Solar: bed area = 11.36 cm^2).

the possibility of singlet oxygen in the TiO_2-photocatalyzed olefin-to-carbonyl oxidative cleavage.

3.2. *TiO_2-catalyzed DPA oxidation with sunlight*

TiO_2 also photocatalyzes the oxidation of DPA to PBQ under natural sunlight in ethanol in the presence of air. The UV–visible spectrum of sunlight illuminated DPA solution in ethanol, in the presence of TiO_2 and air, is similar to that with UV light (λ_{max} = 450 nm). Furthermore, the irradiated solution is EPR silent revealing the absence of diphenylnitroxide. In addition, TLC analysis shows the formation of a single product. Measurement of solar irradiance (W m^{-2}) shows fluctuation of sunlight intensity during the course of the experiment even under clear sky. Hence, the solar experiments at different reaction conditions were carried out in a set so that the quantity of sunlight incident on unit area remains the same. This makes possible comparison of the solar results. A pair of solar experiments carried out simultaneously under identical conditions yield results within ±6% and this is so no different days. The effect of operational parameters on the solar photocatalytic transformation was studied by carrying out the given set of experiments simultaneously and the results presented in each figure represent identical solar irradiance. The PBQ formation rates were obtained by illuminating the DPA solutions on TiO_2 bed for 1 h. The variation of PBQ formation rate with [DPA] is displayed in Fig. 2. The observed increase of PBQ formation with [DPA] is characteristic of Langmuir–Hinshelwood kinetic law. The double reciprocal plot of PBQ formation rate versus [DPA] is linear with a positive y-intercept (figure not given) confirming the Langmuir–Hinshelwood kinetics. Fig. 4 displays the TiO_2-photocatalyzed PBQ formation rate at different airflow rates. The observed enhancement of the reaction by oxygen reveals that the organic transformation conforms to Langmuir–Hinshelwood kinetics with respect to oxygen also. The double reciprocal plot of reaction rate versus airflow rate is a straight line with a finite y-intercept (figure not given). The TiO_2-photocatalyzed PBQ formation was studied without bubbling air but the solution was not deoxygenated. The dissolved oxygen itself brings in the photocatalytic transformation. However, the reaction is slow. The TiO_2-photocatalyzed reaction enhances linearly with the apparent area of TiO_2-bed. Fig. 6 presents the results. PBQ is not formed in the dark. TiO_2 does not lose its photocatalytic efficiency on usage. Reuse of the catalyst shows sustainable photocatalytic activity.

3.3. *Mechanism*

Band gap illumination of TiO_2 generates electron–hole pairs–electrons in the conduction band (CB) and holes in the valence band (VB). The recombination of the electron–hole pairs in semiconductor is so fast (occurring in a picoseconds time scale) and for an effective photocatalysis the reactants are to be adsorbed on the surface of TiO_2 [2]. The hole is likely to take up an electron from the adsorbed DPA molecule to form diphenylamine radical-cation ($Ph_2NH^{\bullet+}$). The oxygen molecule adsorbed on the TiO_2 surface picks up the CB electron. The formed superoxide radical-anion is likely to react with diphenylamine radical-cation yielding PBQ.

$$TiO_2 + h\nu \rightarrow h^+_{(VB)} + e^-_{(CB)}$$

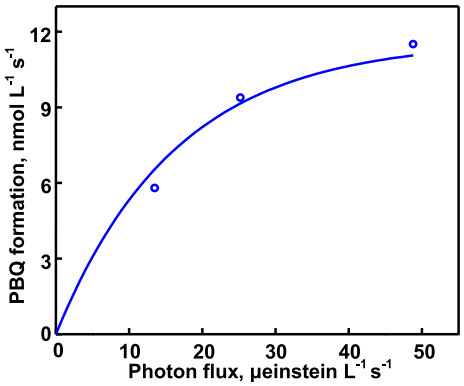

Fig. 5 – Effect of photon flux on TiO_2-photocatalyzed PBQ formation rate ([DPA] = 5.0 mM, TiO_2-loading = 1.0 g, airflow rate = 7.8 mL s^{-1}, λ = 365 nm, volume of reaction solution = 25 mL).

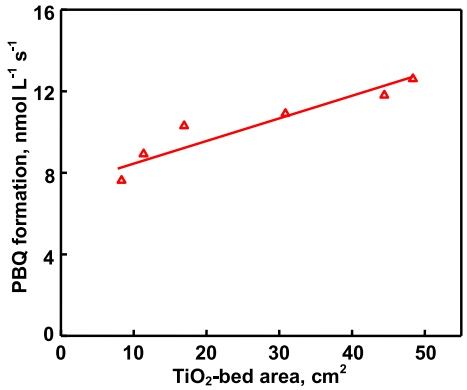

Fig. 6 – TiO_2-photocatalyzed PBQ formation as a function of catalyst-bed area ([DPA] = 5.0 mM, TiO_2-loading = 1.0 g, airflow rate = 4.6 mL s^{-1}, volume of reaction solution = 25 mL).

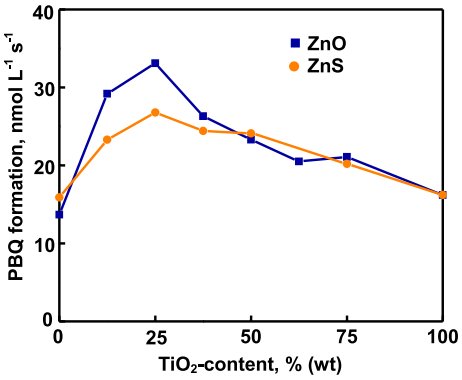

Fig. 7 – Enhanced PBQ formation on mixing TiO_2 with ZnO or ZnS.

$$Ph_2NH_{(ads)} + h^+_{(VB)} \rightarrow Ph_2NH^{\bullet +}$$

$$O_{2(ads)} + e^-_{(CB)} \rightarrow O_2^{\bullet -}$$

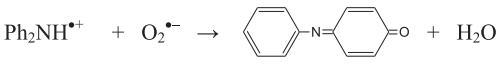

3.4. *Kinetic law*

Kinetic treatment could be made using the results obtained with artificial UV light. The heterogeneous photocatalytic reaction taking place in a continuously stirred tank reactor (CSTR) is governed by the kinetic law [18]:

$$TiO_2\text{-photocatalyzed PBQ formation rate} = kK_1K_2SIC[DPA]\gamma/(1 + K_1[DPA])(1 + K_2\gamma) \quad (1)$$

where K_1 and K_2 are the adsorption coefficients of DPA and O_2 on illuminated TiO_2 surface, k is the specific rate of oxidation of DPA on TiO_2 surface, γ is the airflow rate, S is the specific surface area of TiO_2, C is the amount of TiO_2 suspended per liter and I is the photon flux. The data-fit to the Langmuir–Hinshelwood kinetic curve, drawn using a computer program [18], confirms the rate law (Figs. 2 and 4). The linear double reciprocal plots of TiO_2 formation rate versus [DPA] and airflow rate confirm the kinetic law. The data-fit provides the adsorption coefficients K_1 and K_2 as 56 L mol^{-1} and 0.010 mL^{-1} s, respectively, and the specific reaction rate k as 110 μmol L m^{-2} $einstein^{-1}$. However, the TiO_2-photocatalyzed PBQ formation rate fails to increase linearly with the amount of TiO_2 suspended. This is because of the high catalyst loading. At high catalyst loading, the surface area of the catalyst exposed to light does not commensurate with the weight of the catalyst. The amount of TiO_2 employed is beyond the critical amount corresponding to the volume of the reaction solution and reaction vessel; the whole amount of TiO_2 is not exposed to illumination. The photocatalytic reaction lacks linear dependence on illumination intensity; less than first power dependence of surface-photocatalysis rate on light intensity at high photon flux is well known [19].

3.5. *Enhancement of photooxidation by ZnS and ZnO*

Vectorial transfer of photoformed charge carriers from one semiconductor to another is possible in coupled semiconductors. This separation of charges leads to improved photocatalytic efficiency and examples of coupled semiconductors are many [20]. In coupled semiconductors, both the semiconductors exist in the same particle and the charge separation takes place within the particle. But what we observe here is enhanced photocatalytic transformation of DPA to PBQ on mixing ZnO or ZnS powder with TiO_2 powder. Fig. 7 presents the enhancement of photocatalytic formation of PBQ under UV light on mixing ZnO or ZnS with TiO_2; the two particulate semiconductors are in suspension and at constant motion. This observed enhanced photocatalytic transformation is because of interparticle charge transfer [10,11]. Nanoparticles in suspension aggregate [21]. Fig. 8 presents the particle size distributions of TiO_2, ZnS and ZnO in suspension. Examination of Fig. 8 in conjunction with the determined particle sizes shows aggregation of the particles. As observed in individual semiconductor suspension, aggregation is likely in particulate semiconductor mixtures under suspension and both the semiconductor particles are likely to be present in the aggregates. Charge transfer between TiO_2 and ZnS or ZnO particles is likely to take place when both the semiconductors are under band gap-illumination and in contact with each other; electron from CB of a semiconductor may move to another if the latter is of lower energy and so is the hole from

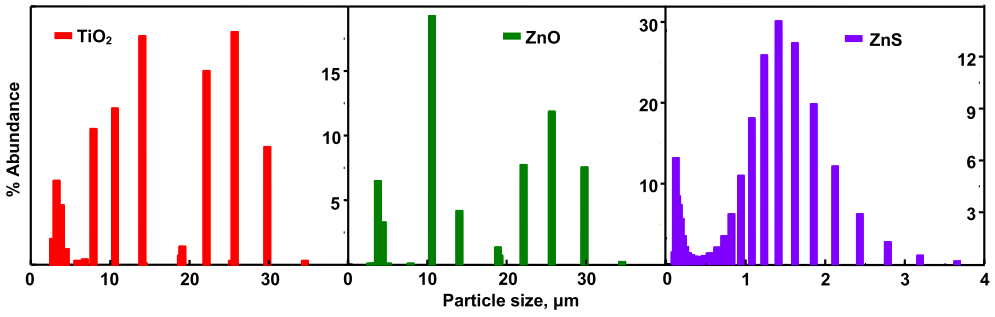

Fig. 8 – Aggregation of nanoparticles.

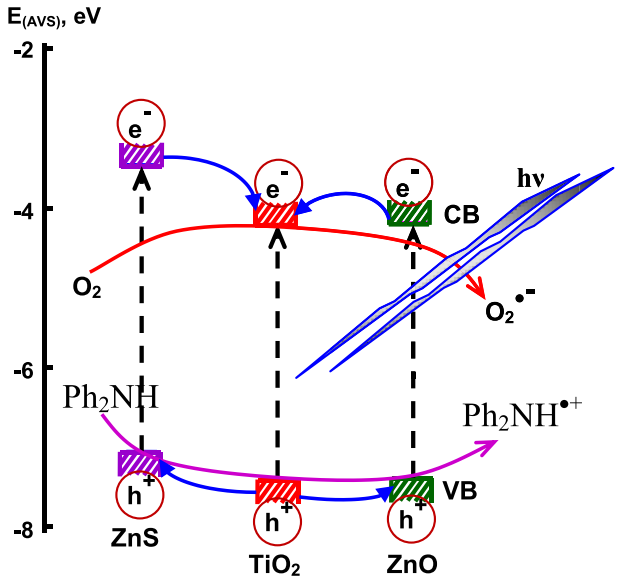

Fig. 9 – Mechanism of enhanced photooxidation.

VB. The charge transfer between the particulate semiconductors is governed by the CB and VB energy levels. The CB electron of TiO_2 is less cathodic than those of ZnO [22] and ZnS [23]. This enables transfer of electron from the CB of ZnO or ZnS to the CB of TiO_2 in TiO_2–ZnO or TiO_2–ZnS mixtures (Fig. 9). The VB hole of TiO_2 is more anodic than those of ZnO and ZnS. This favors transfer of hole from the VB of TiO_2 to that of ZnO or ZnS. This interparticle charge transfer enhances the photocatalytic process. The energy difference between the CB electrons or VB holes of the two semiconductors is the driving force for the interparticle charge separation and the free energy change is given by $-\Delta G = e(E_{(CBSC1)} - E_{(CBSC2)}$ or $e(E_{(VBSC1)} - E_{(VBSC2)})$ [24]. In terms of redox chemistry, the CB and VB refer to the reduced and oxidized states in the semiconductor. In TiO_2 and ZnO or ZnS the CB electrons refer to the reduced forms of Ti^{4+} (*i.e.*, Ti^{3+}) and Zn^{2+} (*i.e.*, Zn^{+}), respectively. Similarly, the VB hole corresponds to the oxidized forms of the respective O^{2-} (*i.e.*, O^{-}) or S^{2-} (*i.e.*, S^{-}). The interparticle charge-transfer, the transfer of electron from the CB of ZnS or ZnO to that of TiO_2 refers to the electron jump from Zn^{+} to Ti^{4+}. The hole-transfer from the VB of TiO_2 to those of ZnO and ZnS corresponds to the electron-jump from O^{2-} of ZnO or S^{2-} of ZnS to O^{-} of TiO_2. The possibility of cross-electron–hole combination, the transfer of electron from the CB of one semiconductor (SC1) to the VB of the other (SC2) is very remote; the very low population of the excited states makes the electron transfer between two excited states highly improbable. A possible reason for not observing the maximum photocatalytic transformation at 50% wt. composition for the semiconductor mixtures is the densities and particle sizes of the semiconductors and also the aggregation.

4. Conclusions

TiO_2 photocatalyzes the oxidative transformation of DPA to BPQ. The BPQ formation enhances with [DPA] and airflow rate and follows the Langmuir–Hinshelwood kinetic law. TiO_2 mixed with ZnO or ZnS produces more PBQ than by the individual semiconductor and this is likely because of interparticle charge separation.

Acknowledgments

Prof. C. Karunakaran is thankful to the Council of Scientific and Industrial Research (CSIR), New Delhi for the Emeritus Scientist Scheme [21(0887)/12/EMR-II].

REFERENCES

[1] Ragesh R, Ganesh VA, Nair SV, Nair AS. A review on 'self-cleaning and multifunctional materials'. J Mater Chem A 2014;2:14773–97.
[2] Xu H, Ouyang S, Liu L, Reunchan P, Umezawa N, Ye J. Recent advances in TiO_2-based photocatalysis. J Mater Chem A 2014;2:12642–61.
[3] Shiraishi Y, Hirai T. Selective organic transformations on titanium oxide-based photocatalysts. J Photochem Photobiol C 2008;9:157–70.
[4] Palmisano G, Garcia-Lopez E, Marci G, Loddo V, Yurdakal S, Augugliaro V, et al. Advances in selective conversions by heterogeneous photocatalysis. Chem Commun 2010;46:7074–89.
[5] Lang X, Chen X, Zhao J. Heterogeneous visible light photocatalysis for selective organic transformations. Chem Soc Rev 2014;43:473–86.
[6] Zanella A. Control of apple superficial scald and ripening – a comparison between 1-methylcyclopropene and diphenylamine postharvest treatment, initial low oxygen stress and ultra low oxygen storage. Postharvest Biol Technol 2003;27:69–78.
[7] Chang YC, Chang PW, Wang CM. Energetic probing for the electron transfer reactions sensitized by 9,10-dicyanoanthracene and 9-cyanoanthracene and their modified zeolite particle. J Phys Chem B 2003;107:1628–33.
[8] Lin TS, Retsky J. ESR studies of photochemical reactions of diphenylamines. J Phys Chem 1986;90:2687–9.
[9] Karunakaran C, Karuthapandian S. Solar photooxidation of diphenylamine. Sol Energy Mater Sol Cells 2006;90:1928–35.
[10] Karunakaran C, Dhanalakshmi R, Gomathisankar P. Semiconductor-photocatalyzed degradation of carboxylic acids: enhancement by particulate semiconductor mixture. Int J Chem Kinet 2009;41:716–26.
[11] Karunakaran C, Dhanalakshmi R, Gomathisankar P, Manikandan G. Enhanced phenol-photodegradation by particulate semiconductor mixtures: interparticle electron-jump. J Hazard Mater 2010;176:799–806.
[12] Karunakaran C, Anilkumar P, Vinayagamoorthy P. Lack of enhanced photocatalytic formation of iodine on particulate semiconductor mixtures. Spectrochim Acta A 2012;98:460–5.
[13] Karunakaran C, Gomathisankar P, Manikandan G. Solar photocatalytic detoxification of cyanide with bactericidal disinfection by oxide ceramics. Indian J Chem Technol 2011;18:169–76.
[14] Adams DM, Raynor JB. Advanced practical inorganic chemistry. New York: John Wiley; 1965.
[15] Puri S, Bansal WR, Sidhu KS. Benzophenone-sensitized photooxidation of diphenylamine. Indian J Chem 1973;11:828.

[16] Bansal WR, Ram N, Sidhu KS. Reaction of singlet oxygen: part I – oxidation of diphenylamine with singlet oxygen ($^1\Delta_g$) produced in situ. Indian J Chem B 1976;14:123–6.
[17] Fox MA, Chen CC. Mechanistic features of the semiconductor photocatalyzed olefin-to-carbonyl oxidative cleavage. J Am Chem Soc 1981;103:6757–9.
[18] Karunakaran C, Senthilvellan S. Semiconductor catalysis of solar photooxidation. Curr Sci 2005;88:962–7.
[19] Vincze L, Kemp TJ. Light flux and light flux density dependence of the photomineralization rate of 2,4-dichlorophenol and chloroacetic acid in the presence of TiO_2. J Photochem Photobiol A 1995;87:257–60.
[20] Karunakaran C, SakthiRaadha S, Gomathisankar P, Vinayagamoorthy P. Nanostructures and optical, electrical, magnetic, and photocatalytic properties of hydrothermally and sonochemically prepared $CuFe_2O_4/SnO_2$. RSC Adv 2013;3:16728–38.
[21] Li M, Noriega-Trevino ME, Nino-Martinez N, Marambio-Jones C, Wang J, Damoiseause R, et al. Synergistic bactericidal activity of Ag-TiO_2 nanoparticles in both light and dark conditions. Environ Sci Technol 2011;45:8989–95.
[22] Lei Y, Zhao G, Liu M, Zhang Z, Tong X, Cao T. Fabrication, characterization, and photoelectrocatalytic application of ZnO nanorods grafted on vertically aligned TiO_2 nanotubes. J Phys Chem C 2009;113:19067–76.
[23] Fan W, Zhang Q, Wang Y. Semiconductor-based nanocomposites for photocatalytic H_2 production and CO_2 conversion. Phys Chem Chem Phys 2013;15:2632–49.
[24] Katoh R, Furube A, Yoshihara T, Hara K, Fujihashi G, Takano S, et al. Efficiencies of electron injection from excited N3 dye into nanocrystalline semiconductor (ZrO_2, TiO_2, ZnO, Nb_2O_5, SnO_2, In_2O_3) films. J Phys Chem B 2004;108:4818–22.